Chemical Physics Letters 582 (2013) 86–89

Contents lists available at ScienceDirect

Chemical Physics Letters

journal homepage: www.elsevier.com/locate/cplett

Counterion-free molecular quantum-dot cellular automata using mixed valence zwitterions – A double-dot derivative of the [*closo*-1-CB_9H_{10}]$^-$ cluster

Yuhui Lu [a,*], Craig S. Lent [b]

[a] Department of Chemistry, Louisiana College, Pineville, LA 71359, United States
[b] Department of Electrical Engineering, University of Notre Dame, Notre Dame, IN 46556, United States

ARTICLE INFO

Article history:
Received 20 May 2013
In final form 9 July 2013
Available online 16 July 2013

ABSTRACT

Molecular quantum-dot cellular automata (QCA) paradigm is a promising approach to molecular electronics. QCA cells can be implemented using mixed-valence compounds. However, the existence of counterions can perturb the local electric field and thus is detrimental to information encoding and processing. Here we examine the feasibility of using charge neutral, zwitterionic mixed-valence complex as QCA cells in which the positive and negative charges are found at different yet fixed locations within the molecule and therefore counterion effects are more predictable and controllable. A double-dot model molecule based on the derivative of the 1-carba-*closo*-decaborate monoanion [*closo*-1-CB_9H_{10}]$^-$ is investigated using computational chemistry techniques. The model molecule demonstrates bistability and switchability.

There has long been great interest in mixed-valence complexes as potential candidates for promising molecular electronic devices [1–3]. One of these potential applications is the quantum-dot cellular automata approach [4]. In the QCA scheme, binary information is represented by the charge configuration of QCA cells, and information transfer is enabled via Coulomb interaction among cells. The principle of QCA has been discussed extensively in the literature [5–9]. Figure 1 schematically shows how binary information can be stored and transferred in the QCA paradigm. At the molecular scale, each QCA cell can be realized using a mixed-valence molecule, by which the quantum dots are provided by redox centers, and binary information is represented by the bistable charge configuration of mixed-valence complexes [10,11]. Several QCA candidate molecules have been synthesized and characterized in the previous studies [12–16], and more candidate molecules are proposed based on theoretical studies [17,18].

One major challenge of using mixed-valence complexes as QCA cells or any other molecular electronic devices is to control the counterion effects. Most mixed-valence complexes are positively charged cations or negatively charged anions, and thus require corresponding counterions to maintain the charge neutrality. These neighboring counterions inevitably disturb the local electric field hence are detrimental to information storage and transport [12]. A natural solution is to use zwitterionic mixed-valence complexes, in which the counterions are covalently built into molecules and positive charge and negative charge are physically separated. The mobile charges that bear binary information are generated via a 'self-doping' mechanism as shown in Figure 2. The advantage of using this type of charge neutral, zwitterionic mixed-valence complexes is that counterions cannot move randomly and therefore their effects are more predictable and controllable.

In our previous report, we investigated the self-doping mechanism using *closo*-hexaborate cluster as the build-in counterion [19]. A dianionic moiety, the *closo*-hexaborate cluster is able to generate two-mobile holes in each QCA cell and thus suitable to be used in four-dot QCA cells. As a proof-of-concept model, our previous study has demonstrated the possibility of charge neutral mixed valence QCA cell. But from a synthetic point of view, to tether four redox centers to four equatorial boron atoms of a *closo*-hexaborate cluster remains challenging, due to the fact that the regioselectivity of this type of compounds has not been thoroughly investigated. Practically, it is relatively more attainable to synthesize a two-dot QCA molecule as shown in Figure 2b. To this end, a monoanionic, instead of a dianionic counterion is needed to build into the molecule. It is well known *closo*-monocarbaborate clusters are monoanionic because a carbon atom has one more valence electron compared to a boron atom [20]. One of the advantages of using *closo*-borate and carbaborate as building blocks is their peculiar solubility and stability. It is known that essentially all salts of the deltahedral polyborate monoacids readily dissolve in electron-donating organic solvent, and the water-soluble salts can be easily extracted into the organic phase [21]. $[B_{10}H_{10}]^{2-}$, $[CB_9H_{10}]^-$, $[B_{12}H_{12}]^{2-}$, and $[CB_{11}H_{12}]^-$ are thermally stable and resistant

* Corresponding author.
E-mail address: lu@lacollege.edu (Y. Lu).

0009-2614/$ - see front matter © 2013 Elsevier B.V. All rights reserved.
http://dx.doi.org/10.1016/j.cplett.2013.07.019

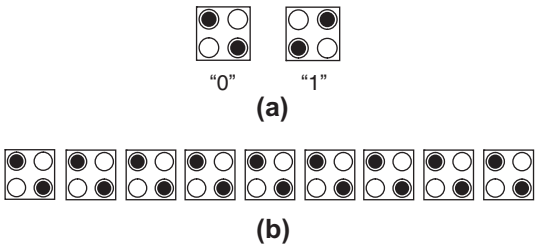

Figure 1. (a) Schematic of a QCA cell. Binary information is encoded in the charge configuration. (b) A QCA wire.

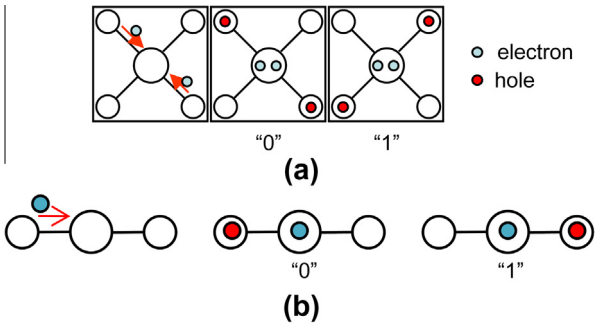

Figure 2. Self-doping mechanism of molecular QCA. (a) A four-dot molecule with a dianionic built-in counterion. (b) A two-dot molecule with a monoanionic built-in counterion.

toward degradation by acids, bases, and mild oxidizing agents [22–24]. In addition, these anions react readily with a variety of reagents to give substitution derivatives [25–28], which opens the door for using them as building blocks in synthetic chemistry. Among various *closo*-monocarbaborate cages, we are especially interested in the 1-carba-*closo*-decaborate monoanion [*closo*-1-CB_9H_{10}]$^-$. It is a good candidate as built-in counterion because its regioselectivity has been explored and pure 1,10-difunctionalized derivatives can be obtained [29,30].

We construct the model molecule *closo*-1-(C≡CC_3H_4)-CB_9H_8-10-(C≡CC_3H_4) to explore the feasibility of this type of double-dot derivative of the [*closo*-1-CB_9H_{10}]$^-$ cluster as QCA cells. Here [*closo*-1-CB_9H_{10}]$^-$ monoanion functions as the build-in counterion which balances the information-bearing mobile charge. Quantum dots are modeled by two allyl (–C_3H_4) groups, which are bound to vertex 1 and 10 of the monocarbaborate cluster via ethynylene (–C≡C–) groups. Allyl is one of the smallest π systems, which has been studied in detail as the quantum dot of QCA molecules [11,31]. The advantage of picking a small redox center like allyl is that the QCA cell so constructed is amenable to high level ab initio computation. The constructed model cell *closo*-1-(C≡CC_3H_4)-CB_9H_8-10-(C≡CC_3H_4) is shown in Figure 3, hereafter denoted as molecule **1**. Our goal is to demonstrate the bistability and switchability of this charge neutral, two-dot mixed valence zwitterionic molecule, using the first principle computational chemistry techniques.

The geometry of the charge neutral, zwitterionic mixed-valence complex *closo*-1-(C≡CC_3H_4)-CB_9H_8-10-(C≡CC_3H_4) is optimized, and harmonic vibrational analysis is conducted to identify the local minima on the PES, for which all frequencies possess only real values. We also confirm the bistability and switchability, two basic requirements for QCA molecules. Computations are implemented using restricted open-shell Hartree–Fock (ROHF) and restricted open-shell Møller–Plesset second-order perturbation (ROMP2) methods to avoid spin contamination. For a comparison, computations were also conducted using the constrained density functional theory (CDFT) [32] with the B3LYP exchange correlation potential. Like conventional density functional theory (DFT) methods, CDFT can treat large molecules with reasonable accuracy without suffering significant spin contamination. It also has the unique advantage of being able to force electrons to localize hence avoid the erroneous electron delocalization caused by the self-interaction error which plagues conventional DFT methods [33]. We have successfully applied the CDFT method to compute STM images of mixed-valence complexes [34–36] as well as the electronic structure of zwitterionic compounds containing *closo*-hexaborate cluster [19]. In this report, the 6-31G* basis set is used for all atoms. ROHF and ROMP2 computations have been done with the MOLPRO program [37], and CDFT computations have been conducted using the NWCHEM program [38].

Molecule **1** has two stable charge configurations, as demonstrated in Figure 4, which shows the electrostatic isopotential surface. The Mulliken charge distribution analysis shows that the charge density is about −1 for the monocarbaborate cluster, +1 for one allyl group, and 0 for other allyl group. The mobile π electron can localize on either allyl group resulting in bistable configurations which can be used to represent binary information '0' and '1'. The optimized geometries of both '0' and '1' states are given in Table 1. The geometrical parameters optimized at ROHF, ROMP2, and CDFT levels are all in good agreement. The most conspicuous difference between the '0' and '1' state is the C–C–C bond angle of allyl groups. The charge neutral allyl radical group has a C–C–C bond angle about 122° while that of the cationic allyl group is about 113°, which are consistent with the allyl bond angles reported in the literature [1,11].

Molecular orbital analysis shows that one unpaired allyl π electron is indeed 'doped' into the monocarbaborate cluster. Figure 5 shows the frontier orbitals of '0' and '1' states of molecule **1**, together with those of the isolated [*closo*-1-CB_9H_{10}]$^-$ monoanion. For the '0' state, the highest occupied molecular orbital (HOMO) localizes on the allyl group bound to the C(1) side of the monocarbaborate cluster. The lowest unoccupied molecular orbital (LUMO) localizes on the other allyl group bound to the B(10) side of the monocarbaborate cluster. The LUMO orbital becomes empty because its electron transfers to the monocarbaborate moiety. For the '1' state, the opposite situation is observed: the HOMO orbital localizes on the B(10) side and the LUMO localizes on the C(1) side.

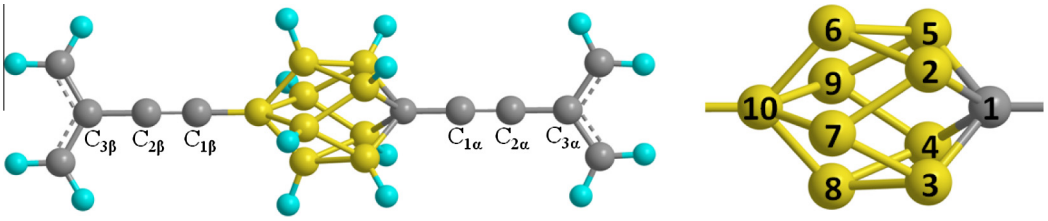

Figure 3. The structure of the model molecule **1**, *closo*-1-(C≡CC_3H_4)-CB_9H_8-10-(C≡CC_3H_4). A *closo*-1-CB_9 monoanion is used as the built-in counterion, and two allyl groups model two active quantum dots. *closo*-1-CB_9 cluster is labeled from 1 to 10.

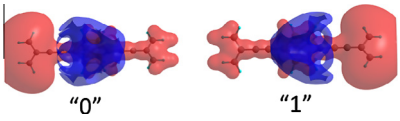

Figure 4. Bistable charge configuration of molecule **1**, *closo*-1-(C≡CC_3H_4)-CB_9H_8-10-(C≡CC_3H_4).The bistability is shown by the electrostatic isopotential surface. The blue surface shows negative charge, and the red surface shows the positive charge. The monocarbaborate cluster, covalently bound inside the molecule, is the negatively charged counterion. Either allyl group can be positively charged. The different charge configurations are used to represent '0' and '1' state. (For interpretation of the references to colour in this figure legend, the reader is referred to the web version of this article.)

Molecular orbital analysis is consistent with the electrostatic isopotential surface shown in Figure 4, from which one can see the allyl group where the LUMO localizes exhibits higher electrostatic potential. For both '0' and '1' state, the HOMO-1 orbitals which largely localize on the monocarbaborate cluster are equivalent to the HOMO orbital of the isolated [*closo*-1-CB_9H_{10}]$^-$ monoanion. The orbital analysis further confirms the self-doping mechanism: the monocarbaborate cluster accepts one electron from an allyl group to obtain a $2n + 2$ (n is the number of vertex of the cluster) electron configuration and satisfies the Wade's rule [39]. The electron donor could be either allyl group therefore resulting in the bistable configuration to encode binary information as discussed above.

Another key requirement of QCA molecules is the switch between the '0' and '1' states driven by the Coulomb perturbation from its neighboring molecules. This switchability is characterized by the cell–cell response function, which is defined as one molecule's polarization as a function of its neighboring molecule's polarization. For a double-dot molecule like **1**, the QCA polarization of the molecule is proportional to its electric dipole moment. The cell–cell response function describes the switching behavior of one QCA cell under the Coulomb interaction of its neighboring cell. To compute the cell–cell response function of **1**, we employ a driver which consists of two positive point charges and one negative point charge, mimicking the presence of a driver molecule, as shown in Figure 6a. The distance between the geometrical center of the point charge driver and that of molecule **1** is fixed at 12 Å, same as the distance between two allyl groups in **1**. The magnitude of the positive driver charge on the both ends is varied smoothly to adjust the dipole moment of the driver D_{driver}. The QCA response function of **1** under the Coulomb interaction of a neighboring molecule, shown in Figure 6b, is the induced molecular dipole moment as a function of the driver dipole moment. The molecular dipole moment is computed for the case of frozen nuclear positions, for which the nuclear coordinates are intermediate between '0' state and '1' state. The intermediate structure is employed such that the computed result can be explained by the electronic structure

Table 1
The optimized structural parameters (in Å) of *closo*-1-(C≡CC_3H_4)-CB_9H_8-10-(C≡CC_3H_4) at ROHF, ROMP2, and constrained DFT/B3LYP levels. Atoms are numbered as shown in Figure 3.

		C_1-B_2	B_{10}-B_9	C_1-$C_{1\alpha}$	B_{10}-$C_{1\beta}$	$C_{2\alpha}$-$C_{3\alpha}$	$C_{2\beta}$-$C_{3\beta}$	C-$C_{3\alpha}$-C	C-$C_{3\beta}$-C
'0'	ROHF	1.608	1.692	1.438	1.548	1.450	1.418	122.0°	113.9°
State	ROMP2	1.615	1.692	1.424	1.511	1.437	1.395	122.5°	112.5°
	CDFT	1.618	1.697	1.426	1.521	1.437	1.420	121.7°	117.3°
'1'	ROHF	1.613	1.707	1.419	1.543	1.420	1.449	114.3°	121.6°
State	ROMP2	1.621	1.711	1.396	1.515	1.396	1.436	112.8°	122.2°
	CDFT	1.623	1.711	1.408	1.521	1.422	1.436	117.6°	121.2°

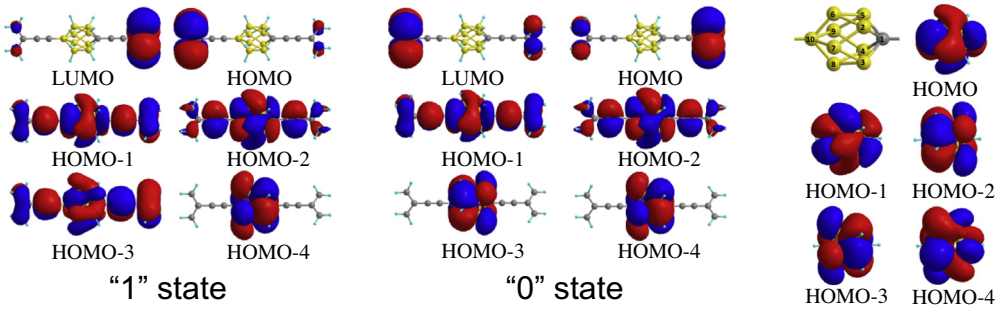

Figure 5. Frontier molecular orbitals of molecule **1**, *closo*-1-(C≡CC_3H_4)-CB_9H_8-10-(C≡CC_3H_4) and the [*closo*-1-CB_9H_{10}]$^-$ monoanion.

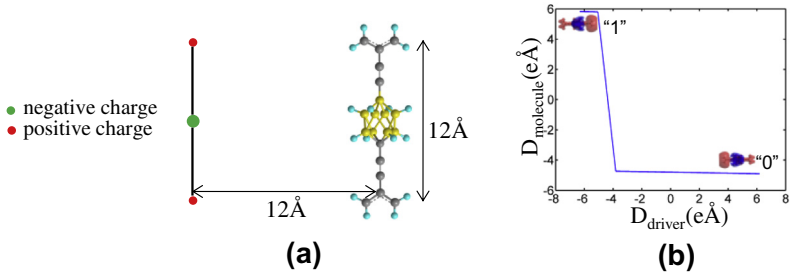

Figure 6. (a) Geometry of the point charge driver used as input to molecule 1. The driver simulates the effect of another nearby molecular cell. (b) The response function of molecule **1** when driven by a neighboring driver.

of the molecule, not by the effect of nuclear relaxation. It is worth noting that the driving force for QCA switching is the Coulomb interaction among neighboring molecules rather than the nuclear relaxation. Nuclear relaxation does play an important role in molecular electron transfer but that effect is secondary for QCA operation. In a previous study, it was found that the electron switch is caused mainly by the change of local field, with only a weak dependence on nuclear relaxation [11]. It is also helpful to note that we do not aim here to study the time-dependent dynamics of QCA switching, but rather to demonstrate the bistability and switchability of model molecule **1** as a charge neutral, zwitterionic QCA cell. A dynamical treatment would go beyond ground state calculations and include thermal excitation effects and scattering mechanisms. Some work has been done in that direction [40].

From Figure 6b one can see that the driver can induce an opposite dipole moment in its neighboring molecule. This means the Coulomb interaction is sufficient to anti-align neighboring molecules thus binary information can be transported in a QCA array via Coulomb interaction, which provides the basis for QCA operation. It should be noted that unlike the symmetric double-dot molecules we previously reported [11,15,40,41], the response function of 1 is not symmetric with respect to the polarization of the driver. For molecule **1** to be switched from '0' to '1' state, a perceptibly negative dipole moment (~ -4 eÅ) must present in the driver. This is because **1** is an uneven double-dot molecule due to the fact that the 1,10-disubstituted derivative of [*closo*-1-CB_9H_{10}]$^-$ cluster is geometrically asymmetric. From the energetic point of view, the eigenenergy of the '0' state is about -0.2 eV lower than that of the '1' state according to the computation at the ROMP2/6–31G* level. This requires a discernible negative dipole moment exhibition in the driver to equalize the '0' and '1' states energetically before the mobile electron can be switched. This unevenness of bistable configuration may be undesirable for implementing the molecular QCA. Nevertheless the above investigation does establish the bistability and switchability of the model molecule **1**, and as a proof-of-concept example it shows that charge neutral, zwitterionic mixed-valence complexes based on the 1,10-disubstituted derivatives of [*closo*-1-CB_9H_{10}]$^-$ cluster has the great potential for molecular QCA.

Acknowledgements

This work was funded by the National Science Foundation through the grant CHE-1124762 and by the Louisiana Board of Regents through the grant LEQSF-EPS(2013)-PFUND-304.

References

[1] A. Aviram, J. Am. Chem. Soc. 110 (1988) 5687.
[2] S. Fraysse, C. Coudret, J.-P. Launay, J. Am. Chem. Soc. 125 (2003) 5880.
[3] S.D. Glover, J.C. Goeltz, B.J. Lear, C.P. Kubiak, Eur. J. Inorg. Chem. 5 (2009) 585.
[4] C.S. Lent, P.D. Tougaw, W. Porod, G.H. Bernstein, Nanotechnology 4 (1993) 49.
[5] A.O. Orlov, I. Amlani, G.H. Bernstein, C.S. Lent, G.L. Snider, Science 277 (1997) 928.
[6] I. Amlani, A.O. Orlov, G. Toth, G.H. Bernstein, C.S. Lent, G.L. Snider, Science 284 (1999) 289.
[7] M. Mitic et al., Appl. Phys. Lett. 89 (2006) 013503.
[8] F. Perez-Martinez, I. Farrer, D. Anderson, G.A.C. Jones, D.A. Ritchie, S.J. Chorley, C.G. Smith, Appl. Phys. Lett. 91 (2007) 032102.
[9] K.K. Yadavalli, A. Orlov, J.P. Timler, C.S. Lent, G.L. Snider, Nanotechnology 18 (2007) 375401.
[10] C.S. Lent, Science 288 (2000) 1597.
[11] C.S. Lent, B. Isaksen, M. Lieberman, J. Am. Chem. Soc. 125 (2003) 1056.
[12] H. Qi, S. Sharma, Z. Li, G.L. Snider, A.O. Orlov, C.S. Lent, T.P. Fehlner, J. Am. Chem. Soc. 125 (2003) 15250.
[13] J. Jiao, G.J. Long, L. Rebbouh, F. Grandjean, A.M. Beatty, T.P. Fehlner, J. Am. Chem. Soc. 127 (2005) 17819.
[14] H. Qi, A. Gupta, B.C. Noll, G.L. Snider, Y. Lu, C.S. Lent, T.P. Fehlner, J. Am. Chem. Soc. 127 (2005) 15218.
[15] Y. Lu, C.S. Lent, J. Comput. Electron. 4 (2005) 115.
[16] V. Arima et al., Nanoscale 4 (2012) 813.
[17] X. Wang, Phys. Chem. Chem. Phys. 13 (2011) 16134.
[18] X. Wang, S. Chen, J. Wen, J. Ma, J. Phys. Chem. C 117 (2013) 1308.
[19] Y. Lu, C.S. Lent, Phys. Chem. Chem. Phys. 13 (2011) 14928.
[20] B. Štíbr, Chem. Rev. 92 (1992) 225.
[21] J. Plešek, Chem. Rev. 92 (1992) 269.
[22] E.L. Muetterties, J.H. Balthis, Y.T. Chia, W.H. Knoth, H.C. Miller, Inorg. Chem. 3 (1964) 444.
[23] S. Körbe, P.J. Schreiber, J. Michl, Chem. Rev. 106 (2006) 5208.
[24] B. Ringstrand, P. Kaszynski, Acc. Chem. Res. 46 (2013) 214.
[25] P. Schleyer, Inorg. Chem 37 (1998) 3454.
[26] T. Jelínek, C.A. Kilner, M. Thornton-Pett, J.D. Kennedy, Chem. Commun. (2001) 1790.
[27] A. Franken, M.J. Carr, W. Clegg, C.A. Kilner, J.D. Kennedy, Dalton Trans. (2004) 3552.
[28] I.B. Sivaev, Z.A. Starikova, P.V. Petrovskii, V.I. Bregadze, S. Sjöberg, J. Organomet. Chem. 690 (2005) 2790.
[29] B. Ringstrand, A. Balinski, A. Franken, P. Kaszynski, Inorg. Chem. 44 (2005) 9561.
[30] B. Ringstrand, P. Kaszynski, V.G. Young Jr., Z. Janoušek, Inorg. Chem. 49 (2010) 1166.
[31] C.S. Lent, B. Isaksen, IEEE Trans. Electron Devices 2003 (1890) 50.
[32] B. Kaduk, T. Kowalczyk, T.V. Voorhis, Chem. Rev. (2012) 112.
[33] A.J. Cohen, P. Mori-Sánchez, W. Yang, Science 321 (2008) 792.
[34] Y. Lu, R. Quardokus, C.S. Lent, F. Justaud, C. Lapinte, S.A. Kandel, J. Am. Chem. Soc. 132 (2010) 13519.
[35] R. Quardokus, Y. Lu, N.A. Wasio, C.S. Lent, F. Justaud, C. Lapinte, S.A. Kandel, J. Am. Chem. Soc. 134 (2012) 1710.
[36] N.A. Wasio et al., J. Phys. Chem. C 116 (2012) 25486.
[37] Werner, H.-J.; Knowles, P.J.; Manby, F.R.; Schütz, M. MOLPRO, Version 2010.1, A Package of ab Initio Programs 2010.
[38] Straatsma, T.P., et al. NWCHEM, A Computional Chemistry Package for Parallel Computers, Version 5.1.1, 2008.
[39] K. Wade, Inorg. Nucl. Chem. Lett. (1972) 8.
[40] Y. Lu, M. Liu, C.S. Lent, J. Appl. Phys. 102 (2007) 034311.
[41] Y. Lu, C.S. Lent, Nanotechnology 19 (2008) 155703.